

Coaxial Twin-shaft Magnetic Fluid Seals Applied in Vacuum Wafer-Handling Robot

CONG Ming^{1,*}, WEN Haiying¹, DU Yu¹, and DAI Penglei²

¹ School of Mechanical Engineering, Dalian University of Technology, Dalian 116023, China

² Sany Heavy Equipment Co., Ltd, Shenyang 110141, China

Received June 23, 2011; revised March 29, 2012; accepted April 5, 2012

Abstract: Compared with traditional mechanical seals, magnetic fluid seals have unique characters of high airtightness, minimal friction torque requirements, pollution-free and long life-span, widely used in vacuum robots. With the rapid development of Integrate Circuit (IC), there is a stringent requirement for sealing wafer-handling robots when working in a vacuum environment. The parameters of magnetic fluid seals structure is very important in the vacuum robot design. This paper gives a magnetic fluid seal device for the robot. Firstly, the seal differential pressure formulas of magnetic fluid seal are deduced according to the theory of ferrohydrodynamics, which indicate that the magnetic field gradient in the sealing gap determines the seal capacity of magnetic fluid seal. Secondly, the magnetic analysis model of twin-shaft magnetic fluid seals structure is established. By analyzing the magnetic field distribution of dual magnetic fluid seal, the optimal value ranges of important parameters, including parameters of the permanent magnetic ring, the magnetic pole tooth, the outer shaft, the outer shaft sleeve and the axial relative position of two permanent magnetic rings, which affect the seal differential pressure, are obtained. A wafer-handling robot equipped with coaxial twin-shaft magnetic fluid rotary seals and bellows seal is devised and an optimized twin-shaft magnetic fluid seals experimental platform is built. Test result shows that when the speed of the two rotational shafts ranges from 0–500 r/min, the maximum burst pressure is about 0.24 MPa. Magnetic fluid rotary seals can provide satisfactory performance in the application of wafer-handling robot. The proposed coaxial twin-shaft magnetic fluid rotary seal provides the instruction to design high-speed vacuum robot.

Key words: magnetic fluid, seals, coaxial twin-shaft, magnetic field, wafer handling robot

1 Introduction

Generally, a wafer-handling robot works in vacuum chamber or other non-atmospheric environments^[1]. For example, in semiconductor fabrication, substrates or wafers may need to be moved in and out of processing chambers by the wafer-handling robot in a vacuum or near-vacuum environment^[2]. To isolate pollution source from the vacuum chamber, a reliable hermetical technique is crucial for wafer-handling robots^[3].

Magnetic fluid rotary seals have been shown to be effective for rotary shafts operating in a vacuum chamber^[4]. Magnetic fluid sealing technology is a research hotspot in the world as a foreland topic. The transmission of rotary motion with this method has the following advantages: zero leakage at high speed, minimal friction torque requirements, minimal contamination level, and no maintenance required^[5].

Works on the factors that affect the seal differential pressure have been done by many scholars. BRAS, et al^[6], designed a new structure of magnetic fluid sealing using bilateral assembled magnetism, which can form a 0.5 T magnetic field between the pole shoes and rotating shaft. But this structure needs a high technological requirements and producing strong magnetic flux leakage. OZAKI, et al^[7], discovered there is a optimal value in both magnetic field strength and magnetic fluid quantity. The sealing ability raises first and then descends as the value increases. JIM^[8] reached a conclusion that sealing pressure differential is proportional to the magnetic induction when seal gap is a fixed value through a single-stage shaft sealing experiment.

As an important kind of wafer-handling robot, the R - θ robot has 3 DOF, R (radial linear) movement, θ (rotary) movement and Z (vertical) movement, to fulfill the mission of transferring wafer among processing units in vacuum environment^[9]. To achieve the DOF of R and θ , two rotational motions need to be transmitted from atmosphere to vacuum chamber by the aid of reliable rotary sealing device^[10]. Then, pulleys and belts are used to drive the robot arms to achieve the desired motion. It's obvious that

* Corresponding author. E-mail: congm@dlut.edu.cn

This project is supported by National Natural Science Foundation of China (Grant No. 50675027)

© Chinese Mechanical Engineering Society and Springer-Verlag Berlin Heidelberg 2012

magnetic fluid seal is a good choice for rotary hermetic seal of wafer-handling robots^[11]. In this paper, an $R-\theta$ robot is devised, and the design optimization of coaxial twin-shaft magnetic fluid rotary seals is introduced emphatically.

2 Magnetic Fluid Seals

The common structure of monaxial magnetic fluid rotary seals is shown in Fig. 1. The device normally consists of bearings, magnetic pole pieces, permanent magnetic ring, magnetically permeable rotary shaft and magnetic fluid^[5, 12]. The working principle is as follows: The magnetic pole pieces, the permanent magnetic ring, and the magnetically permeable rotary shaft compose a closed magnetic circuit. Because of the magnetic energy in the permanent magnetic ring, a strong magnetic field is generated in the gaps between rotary shaft and magnetic pole pieces, and holds the magnetic fluid in gaps tightly. The magnetic fluid kept in gaps forms "O"-rings, which lock gaps and achieve sealing^[13-14]. When the magnetic fluid seal makes isolation for the two chambers whose pressures are different, it's the magnetic fluid that withstands the superfluous pressure. With the increasing of superfluous pressure, the sealing becomes difficult^[7].

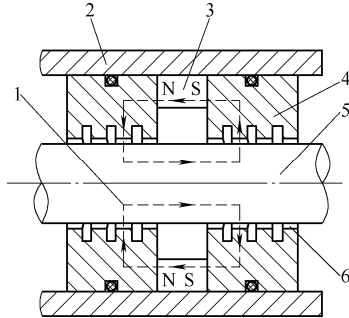


Fig. 1. Typical structure of monaxial magnetic fluid rotary seals:

1. Agnetic circuit 2. Housing 3. Permanent magnetic ring
4. Pole piece 5. Rotary shaft 6. Magnetic fluid

In general, magnetic fluid is treated as continuous and incompressible, and according to the ferrohydrodynamic analysis, the ferrohydrodynamic Bernoulli equation^[15] is represented as follows:

$$p^* + \frac{1}{2} \rho v^2 + \rho gh - \int_0^B M(B) dB = C, \quad (1)$$

where p^* —Pressure in the magnetic fluid,
 v —Flow velocity,
 M —Magnetization of magnetic fluid,
 B —Magnetic flux density,
 g —Acceleration of gravity,
 ρ —Density of magnetic fluid,
 h —Height measured relative to the reference level for the gravitational potential,
 C —Constant value under a certain condition.

The seal pressure differential between high pressure side and low pressure side, with reference to Fig. 2, can be maintained under a rotating shaft condition.

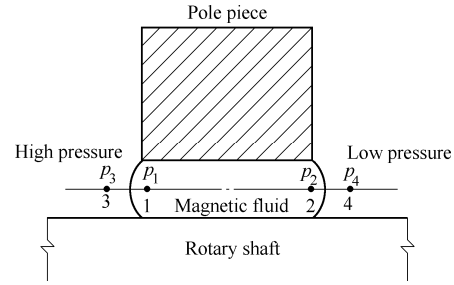


Fig. 2. Microcosmic schematic diagram of magnetic fluid rotary seals

The seal pressure differential $\Delta p = p_3 - p_4$ can be estimated by the static equilibrium Eq. (1), assuming that the gravitational force is ignored and the magnetic fluid in the sealing gap is in a static state with a condition of the magnetic field being tangential at the interface. With the magnetic condition at the interface, there would be no magnetic pressure jump, so that $p_1^* = p_3$ and $p_2^* = p_4$. Thus, the seal pressure differential can be estimated by^[16]

$$\Delta p = p_3 - p_4 = p_1^* - p_2^* = \int_{B_1}^{B_2} M(B) dB. \quad (2)$$

Where B_1 and B_2 are the values of the magnetic flux density on the left and right surface respectively. Δp is a pressure differential held by one stage of the magnetic fluid seals. When B_1 reaches the maximum value B_{\max} and B_2 reaches the minimum value B_{\min} and the total magnetic fluid is in the saturation, a differential pressure sustained by the seal reaches the maximum:

$$\Delta p_{\max} = \int_{B_{\min}}^{B_{\max}} M_s dB = M_s (B_{\max} - B_{\min}). \quad (3)$$

Based on Eq. (3), we can obtain the seal differential pressure formulas as follows:

$$\Delta p_{\text{total}} = M_s \sum_{i=1}^N [(B_{\max})_i - (B_{\min})_i], \quad (4)$$

where Δp_{total} —Maximum burst pressure sustained by the magnetic fluid rotary seals,
 M_s —Saturation magnetization of magnetic fluid,
 N —Number of seal stages,
 B_{\max} —Maximal values of the magnetic flux density in the magnetic fluid,
 B_{\min} —Minimal values of the magnetic flux density in the magnetic fluid.

Eq. (4) shows that the maximum seal pressure

differential can be increased by optimizing the following parameters:

First, the number of seal stages N should be as large as possible. But a large number of seal stages will result in complicated structures. In addition, for the same seal length, a high N value will result in a relative high value for B_{\min} which will reduce the gain in seal pressure per seal step. Therefore, we choose eight stage seals in the design of this paper.

Second, the material constant M_s should be as high as possible. But the magnetic fluid with high M_s will bring a high cost in the design of sealing device. In this research we choose a lower vapor pressure magnetic fluid with saturation magnetization $M_s = 30$ kA/m.

The last parameter is $B_{\max} - B_{\min}$. Using finite element simulations of the magnetic flux density within the sealing gap, we can optimize this parameter by varying structure parameters of magnetic rotary seals, and this is what we investigate in this paper^[17].

3 Parameter Optimization of Twin-shaft Magnetic Fluid Seals structure

The generic structure of coaxial twin-shaft magnetic fluid rotary seals is shown in Fig. 3. The main factors that influence the sealing performance are the parameters of the permanent magnetic ring, the magnetic pole tooth, the outer shaft and the outer shaft sleeve. Besides, the axial relative position of two permanent magnetic rings also plays a significant role. Optimizing the structure parameters of the above factors is significant for getting a high $B_{\max} - B_{\min}$ which determines the sealing property of coaxial twin-shaft magnetic fluid rotary seals. In this paper, we use the control variable method to optimize the structure parameters of sealing device.

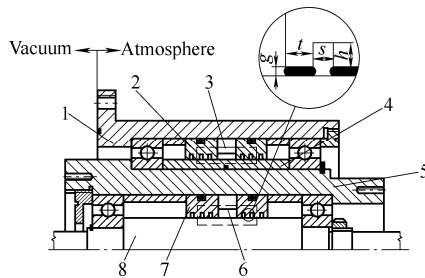


Fig. 3. Generic structure of coaxial twin-shaft magnetic fluid rotary seals:

1. Magnetism isolating housing
2. Outer magnetic poles
3. Outer permanent magnetic ring
4. Magnetic conductive outer shaft sleeve
5. Magnetism isolating outer shaft
6. Inner permanent magnetic ring
7. Inner magnetic poles
8. Magnetic conductive inner shaft

The seal model constructed by us is two-dimensional and axis-symmetrical, which includes NdFeB magnet (the permanent magnet), stainless steel (pole piece and inner

shaft), aluminum (sleeve and outer shaft) and atmosphere. The material parameters for NdFeB are: the remanent magnetic induction $B_r = 1.20$ T, the coercivity $H_c = 935$ kA/m, and the differential permeability is 1.02. The grade of stainless steel is No.10 and its B-H curve is shown in Fig. 4. As magnetism isolating material, aluminum's differential permeability is 1.00, which is the same as that of atmosphere.

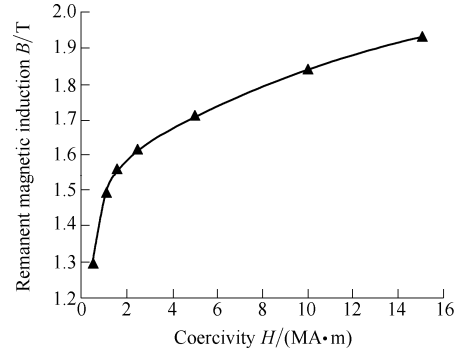


Fig. 4. B-H curve of 10# steel

3.1 Permanent magnetic ring

The permanent magnet used in the model is NdFeB magnet. The main parameters of permanent magnetic ring are inner diameter D_i , outer diameter D_o , and axial length L_m . The maximum magnetic flux density in sealing gaps is influenced heavily by the dimensions of permanent magnetic ring. For that reason, it is of great significance to find the rational dimensions of permanent magnetic ring to ensure the pressure resisting ability of the sealing device.

3.1.1 Axial length L_m

In the calculation, we only change the axial length of the permanent magnetic ring (L_m) and other parameters of the sealing device remain unchanged. The magnetic field intensity distribution in sealing gaps of inner and outer shaft is calculated by finite element method. Fig. 5 shows the seal pressure differential curve. When the axial length grows to a certain value, the sealing capability remains unchanged. The sealing capability of the inner and outer shaft increases gradually with the growth of the axial length of permanent magnetic ring. As a result, selecting a suitable axial length of the permanent magnetic ring can not only decrease the axial length of the sealing device, but raise the utilization rate of the permanent magnet as well. When the sealing gap g is 0.2 mm, the axial length of the permanent magnetic ring L_m can be 10–15 mm.

3.1.2 Inner diameter D_i and Outer diameter D_o

The inner diameter of the permanent magnetic ring can be determined by the diameter of the corresponding shaft. The inner permanent magnetic ring corresponds to inner shaft and the outer permanent magnetic ring corresponds to flux sleeve. When the inner diameters of the inner and outer permanent magnetic rings are 10–14 mm larger than the outer diameters of the inner shaft and flux sleeve respectively, the magnetic flux leakage is less.

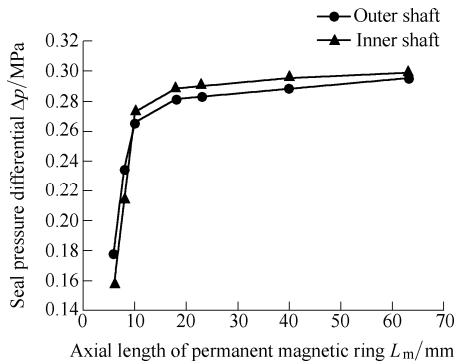


Fig. 5. Seal pressure differential versus axial length of permanent magnetic ring

Method of trials and errors is used by selecting the outer diameter of the permanent magnetic ring. We use magnetic finite element method to calculate the seal pressure differential by changing D_o gradually. We keep L_m and D_i invariable, before we get the desired seal pressure differential. In this way we get the value of the outer diameter D_o .

3.2 Magnetic pole tooth

When the dimensions of the permanent magnetic ring are fixed, the magnetic field distribution in the sealing gap is determined by the tooth parameters including the sealing gap g , the tooth width t , the slot width s and the tooth height h . The magnetic pole tooth structure is shown in Fig. 3.

3.2.1 Sealing gap g

Fig. 6 illustrates the relationship of the seal pressure differential and the sealing gap. When the sealing gap is increased, the seal pressure differential of inner and outer shaft will both decrease gradually. Thus, it is easy to see that the sealing gap should be as small as possible. Generally the value of sealing gap g can range from 0.1 mm to 0.3 mm.

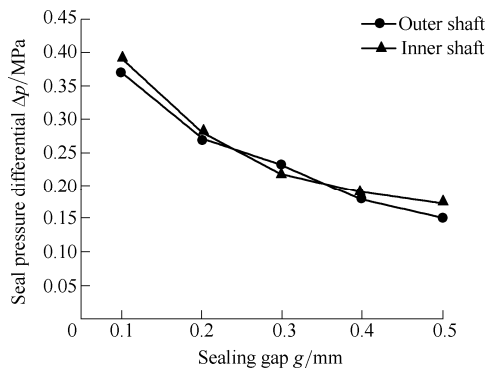


Fig. 6. Seal pressure differential versus sealing gap

3.2.2 Tooth parameters

The tooth parameters include the tooth width t , the slot width s and the tooth height h . Fig. 7 to Fig. 9 illustrate the relationship of the seal pressure differential and tooth parameters. The tooth width affects the maximum flux

density (B_{\max}) under a tooth, while the slot width and the tooth height affect the minimum flux density (B_{\min}) under a slot and in the seal gap respectively. Accordingly, the seal pressure differential varies with the value of $B_{\max} - B_{\min}$ (Eq. (4)). The calculation results show that the optimum ranges of tooth parameters are as follows: $t=0.6-1.2$ mm, $s=2-5$ mm, $h=1-3$ mm.

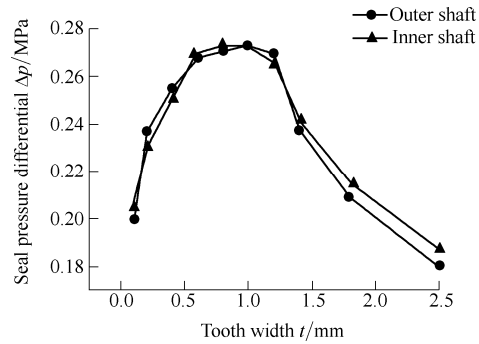


Fig. 7. Seal pressure differential versus tooth width

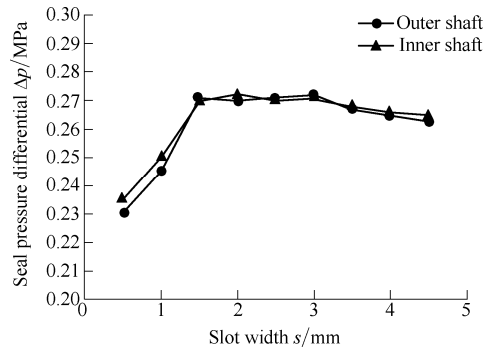


Fig. 8. Seal pressure differential versus slot width

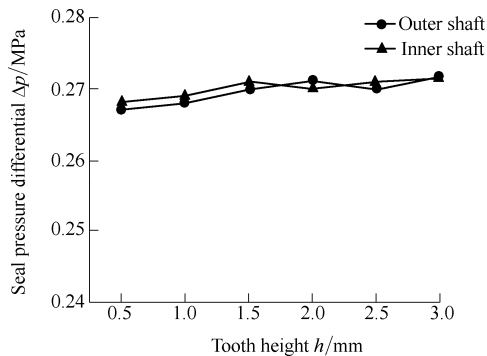


Fig. 9. Seal pressure differential versus tooth height

3.3 Outer shaft and the outer shaft sleeve

3.3.1 Magnetism isolating outer shaft

Fig. 3 shows that the inner diameter of the outer shaft and the outer diameter of the inner permanent magnetic ring are equal in size, so the inner diameter of the outer shaft is determined by the size of permanent magnetic ring. The outer diameter can be determined by the radial thickness of the outer shaft a , so the radial thickness is a

key parameter of the outer shaft design.

The function of magnetism isolating outer shaft is to insulate the mutual influence between magnetic fields generated by inner and outer magnetic rings. If the radial thickness of outer shaft is too small, the influence between magnetic fields will become severe and the inner Δp_{total} will be small. On the other hand, an oversize outer shaft will add the radial size of the whole sealing device. So it is very important to choose a right size for magnetism isolating outer shaft. Fig. 10 illustrates the relationship of the inner seal pressure differential and the radial thickness of outer shaft when the radial thickness of shaft sleeve is 6 mm. From the analysis we can get the reasonable range of the radial thickness of the outer shaft a which is 9–11 mm.

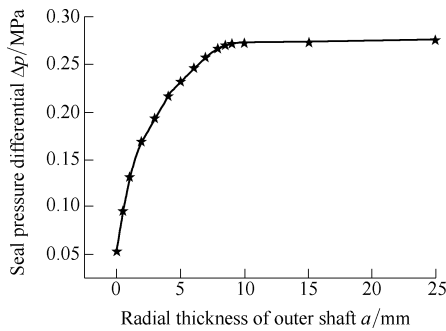


Fig. 10. Seal pressure differential versus wall thickness of outer shaft

3.3.2 Magnetic conductive outer shaft sleeve

Similarly, the radial thickness size of outer shaft sleeve b is the key parameter. Magnetic conductive outer shaft sleeve's function is to permit transit of magnetism and ensure an adequate magnetic field in the sealing gaps. A right radial thickness size of outer shaft sleeve can insure a high outer Δp_{total} and pinch the radial size of sealing device. Fig. 11 illustrates the relationship of the outer seal pressure differential and the radial thickness of outer shaft sleeve when the radial thickness of outer shaft is 10 mm. We get the reasonable range of b which is 8–10 mm.

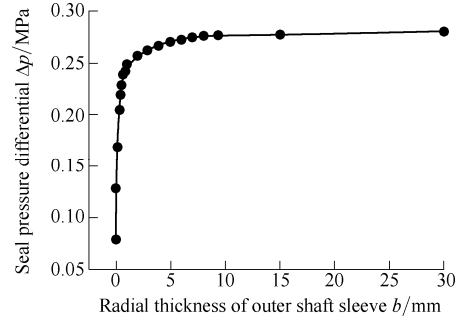


Fig. 11 Outer seal pressure differential versus radial thickness of outer shaft sleeve

3.4 Relative position of two permanent magnetic rings

As magnetic fields generated by inner and outer permanent magnetic rings affect with each other, the axial relative position of two rings is an important factor that influences sealing performance. In this paper, four different models shown in Fig. 12 are analyzed by the software of ANSYS10.0. The analyzing results are presented in Table 1.

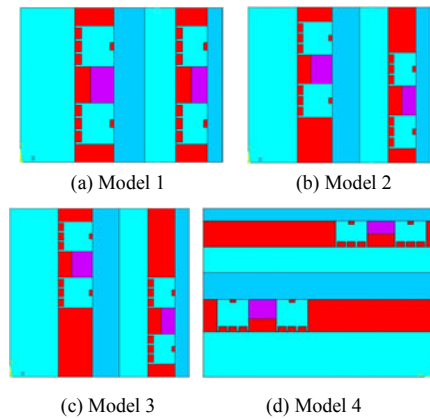


Fig. 12 Four different models of dual magnetic fluid seal

From Table 1, we can summarize that model 1 has relative poor hermetic performance compared with the other three models. The differential of Δp_{total} between model 2, 3 and 4 is small. Considering the axial size of sealing device, we choose model 2 as final design.

Table 1. Analysis results of four magnetic fluid seal models

No.	Inner shaft			Outer shaft		
	Magnetic flux density $\Sigma B_{\text{max}}/\text{T}$	Magnetic flux density $\Sigma B_{\text{min}}/\text{T}$	Pressure differential $\Delta p_{\text{inner}}/\text{MPa}$	Magnetic flux density $\Sigma B_{\text{max}}/\text{T}$	Magnetic flux density $\Sigma B_{\text{min}}/\text{T}$	Pressure differential $\Delta p_{\text{outer}}/\text{MPa}$
1	12.589	3.884	0.261	10.215	1.682	0.256
2	12.869	3.836	0.271	10.553	1.612	0.268
3	12.883	3.801	0.272	10.576	1.559	0.270
4	12.911	3.769	0.274	10.618	1.541	0.272

4 Analysis and Experimental Results of Sealing Structure

4.1 Seals structure

To achieve the DOF of R and θ , two rotational motions

need to be transmitted from atmosphere to vacuum chamber. The final design of coaxial twin-shaft magnetic fluid rotary seals for wafer-handling robots is illustrated in Fig. 13. The static seal of this structure is used of O-shape seal ring. The saturation magnetization of magnetic fluid M_s is 30 kA/m and the permanent magnet is NdFeB N40. Remanent

magnetic induction $B_r = 1.20$ T and coercivity $H_c = 935$ kA/m. The structure parameters of this device are shown in Table 2.

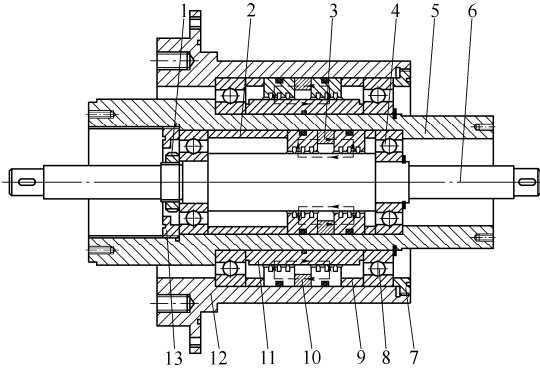


Fig. 13 Final structure of coaxial twin-shaft magnetic fluid rotary seals

1. Nut 2. Inner sleeve
3. Magnetic fluid rotary seals of inner shaft
4. Bearing of inner shaft 5. Magnetism isolating outer shaft
6. Inner shaft 7. Outer end cover 8. Bearing of outer shaft
9. Outer sleeve 10. Magnetic fluid rotary seals of outer shaft
11. Magnetic conductive sleeve of outer shaft
12. Magnetism isolating housing 13. Inner end cover

Table 2. Parameters of twin-shaft magnetic fluid seals

Structure parameter	Inner shaft	Outer shaft
Inner diameter of shaft D_{in}/mm	0	60
Outer diameter of shaft D_{ou}/mm	35	80
Inner diameter of permanent magnet D_{pmin}/mm	45	110
Outer diameter of permanent magnet D_{pmou}/mm	60	120
Sealing gap g/mm	0.2	
Tooth width t/mm	1	
Slot width s/mm	2	
Tooth height h/mm	2	
Axial length of permanent magnet L_m/mm	12	
Radial thickness of outer shaft sleeve a/mm	9	
Stage number	8	

4.2 Analysis and experimental results

By analyzing the proposed sealing device, we can get the distribution of the magnetic flux density in the sealing gaps under the pole pieces is shown in Fig. 14. According to Eq. (4), the seal capacity can be numerated on the basis of magnetic field distribution. The ΔP_{total} of inner and outer shaft can be calculated as follows.

Inner shaft:

$$\Delta p_{\text{total}} = \sum_{i=1}^8 M_s (B_{\text{max}} - B_{\text{min}}) = M_s \left(\sum_{i=1}^8 B_{\text{max}} - \sum_{i=1}^8 B_{\text{min}} \right) = 3 \times 10^4 \times (12.83 - 3.72) = 0.273(\text{MPa}).$$

Outer shaft:

$$\Delta p_{\text{total}} = \sum_{i=1}^8 M_s (B_{\text{max}} - B_{\text{min}}) = M_s \left(\sum_{i=1}^8 B_{\text{max}} - \sum_{i=1}^8 B_{\text{min}} \right) = 3 \times 10^4 \times (10.43 - 1.61) = 0.265(\text{MPa}).$$

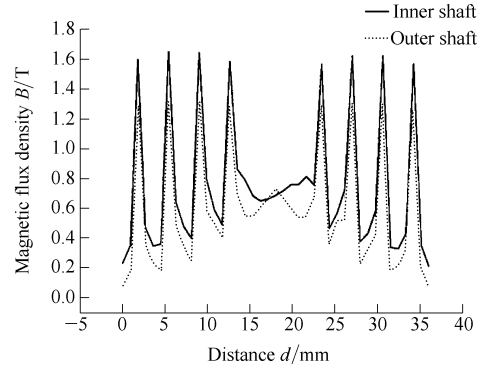


Fig. 14 Magnetic flux density distribution in sealing gap for inner and outer shaft

The sealing test of the device is made. This test has mainly measured the maximum burst pressure Δp_{total} of the coaxial twin-shaft magnetic fluid rotary seals device under the running state. We can get the seal pressure differential by subtracting one atmosphere from the greatest burst pressure. The experiment device consists of Pneumatic equipment, magnetic fluid rotary seals structure and drive unit. The structure of the device is shown in Fig. 15.

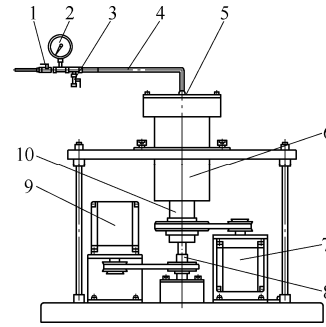


Fig. 15 Structure of the twin-shaft magnetic fluid rotary seals experiment device

1. Switch valve 2. Pressure gauge 3. Bleed valve
4. Air pipe 5. Seal end plate 6. Magnetism isolating housing
7. Outer shaft stepper motor 8. Inner shaft
9. Inner shaft stepper motor 10. Magnetism isolating outer shaft

We make the inner shaft and the outer shaft rotate at the same speed and use the air pipe to inject high pressure gas into the sealing devices. Then we can detect and record the maximum burst pressure at this speed. For reflecting the real operation, the speed of the two shafts is changed in each test. The seal pressure differential at different speed is obtained by using the above method. Fig. 16 shows the seal pressure differential when the speed of the two rotational shafts ranges from 0 r/min to 500 r/min. The experimental results indicate that the rotational velocity has little influence on the sealing ability when the shafts are at low speed.

The wafer-handling robot works in vacuum environment and the pressure is 10–6 Pa, while the outside of the cluster tools is at standard atmospheric pressure. Thus the magnetic fluid seal device needs to sustain one standard

atmosphere pressure. From the experiment above, we know that the Δp_{total} of inner and outer shaft are all about 0.24 MPa. The coaxial twin-shaft magnetic fluid rotary seals designed in this paper can meet the sealing requirements of vacuum in wafer processing system.

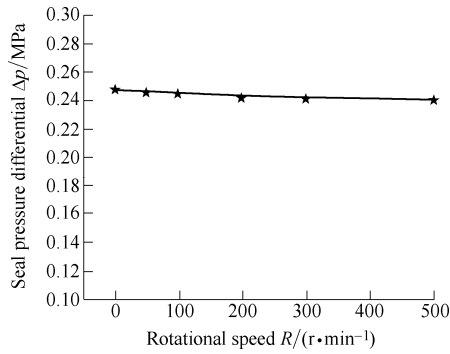


Fig. 16 Seal pressure differential versus rotational speed for Twin-shaft magnetic fluid seal structure

5 Wafer-Handling Robot Equipped with Coaxial Twin-shaft Magnetic Fluid Rotary Seals

The wafer-handling robot designed in this paper belongs to the polar coordinate robot and can achieve R (radial linear) movement, θ (rotary) movement and Z (vertical) movement. R, θ and Z movements are driven by AC servomotors. The robot can hold wafer with vacuum suction system^[15].

To realize R and θ movements of the robot, the torques of two AC servomotors are transferred into vacuum by the aid of coaxial twin-shaft magnetic fluid rotary seals. Fig. 17 shows the R movement of the robot. The AC servomotor connects to the outer shaft of seal device by harmonic reducer and isochronous cincture, and the upper side of outer shaft is connected to the back arm body directly. So the R movement can be achieved by the rotation of AC servomotor of outer shaft. The θ movement for wafer-handling robots is shown in Fig. 18. When the two driving AC servomotors rotate in the same direction and at the same speed, the torques will be transferred into the inner and outer shafts of seal device respectively and then the big belt pulley and the back arm body attached to the seal shafts will rotate at the same speed. The θ movement of robot is achieved.

The function of Z movement is to adjust the vertical position of wafer hand when the robot takes or puts wafer during processing. When the vertical movement is transferred from atmosphere to vacuum, a reliable linear seal device is also needed to isolate pollution source from the vacuum chamber. As a simple and effective linear seal structure, bellows seal can perform a good linear seal property under the condition of several atmospheric

intensity of pressure. In this design, the bellows seal is used to fulfill the sealing requirement of Z movement. Fig. 19 shows the Z movement of the wafer-handling robot. The bellows seal encloses the coaxial twin-shaft magnetic fluid rotary seals, forming a three shafts sealing structure which is attached to the movable platform by draw-bars. By the aid of screw-nut pairs and isochronous cincture, the rotary movement of AC servomotor is transformed into vertical movement of movable platform. As the three shafts sealing structure move vertically with the movable platform, the Z movement of robot is realized.

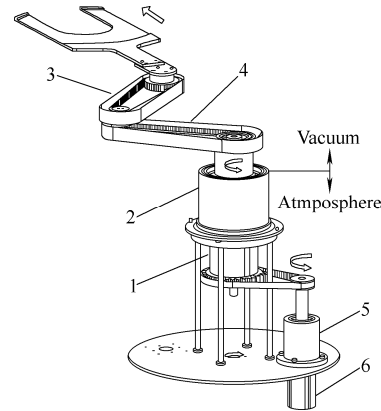


Fig. 17. Descriptive diagram for R movement of wafer-handling robot

1. Outer shaft 2. Coaxial twin-shaft magnetic fluid rotary seals
3. Forearm 4. Back arm 5. Harmonic reducer of outer shaft
6. AC servomotor of outer shaft

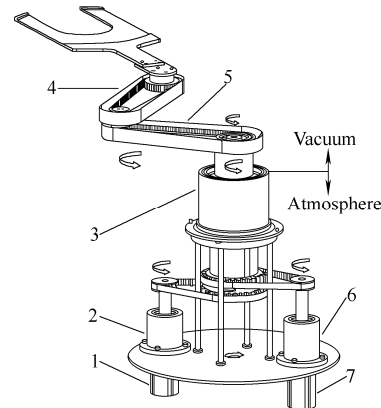


Fig. 18. Descriptive diagram for θ movement of wafer-handling robot

1. AC servomotor of inner shaft
2. Harmonic reducer of inner shaft
3. Coaxial twin-shaft magnetic fluid rotary seals
4. Forearm 5. Back arm
6. Harmonic reducer of outer shaft
7. AC servomotor of outer shaft

Fig. 20 shows the overall structure of the wafer-handling robot. The robot can achieve radial linear movement, rotary movement and vertical movement to fulfill the mission of transferring wafer in vacuum chamber or other non-atmospheric environments.

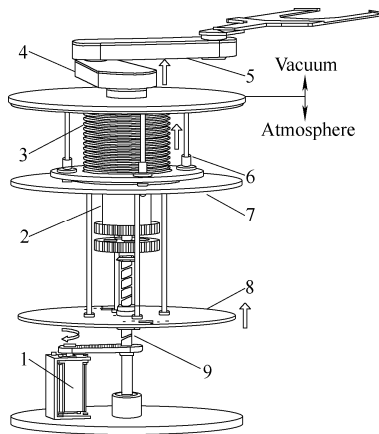


Fig. 19. Descriptive diagram for Z movement of wafer-handling robot

1. AC servomotor of screw 2. Outer shaft
3. Bellows seal 4. Back arm 5. Forearm
6. Linear bearing 7. Immovable platform
8. Movable platform 9. Screw

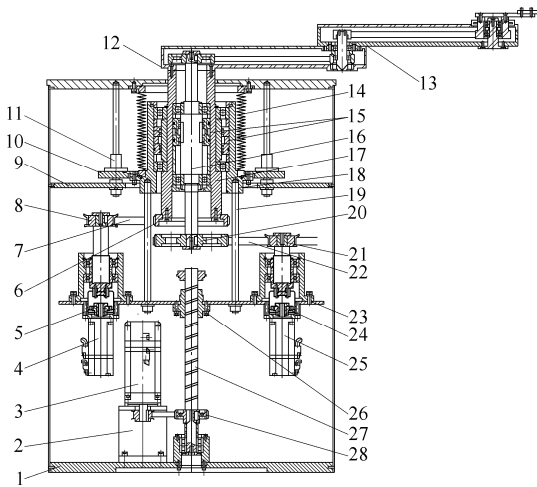


Fig. 20. Overall structure of wafer-handling robot

1. Base 2. Holder of servomotor 3. Lift AC servomotor
4. AC servomotor of outer shaft
5. Harmonic reducer of outer shaft
6. Big belt pulley of outer shaft
7. Isochronous cincture of outer shaft
8. Small belt pulley of outer shaft
9. Immovable platform 10. Lift plate
11. Linear bearing 12. Driving end of back arm
13. Subassembly of robot arm 14. Bellows seal
15. Magnetic fluid rotary seals 16. Inner shaft
17. Outer shaft 18. Sleeve 19. Draw-bar
20. Big belt pulley of inner shaft
21. Small belt pulley of inner shaft
22. Isochronous cincture of inner shaft
23. Movable platform 24. Harmonic reducer of inner shaft
25. AC servomotor of inner shaft 26. Screw-nut
27. Screw 28. Belt pulley of screw

6 Conclusions

(1) By analyzing the magnetic field distribution of dual magnetic fluid seal, the optimal value ranges of important parameters which affect the seal differential pressure are obtained, including parameters of the permanent magnetic ring, the magnetic pole tooth, the outer shaft, the outer shaft

sleeve and the axial relative position of two permanent magnetic rings.

(2) A coaxial twin-shaft magnetic fluid rotary seals is devised by parameter design of the structure, which has high sealing capability and can commendably meet the sealing requirements of wafer processing system.

(3) A wafer-handling robot equipped with above seals is designed. It can enhance the grade of vacuum and cleanliness of wafer manufacturing environment. By using the most advanced magnetic fluid technology and seal design technology, magnetic fluid rotary seals can provide satisfactory performance in the new challenging application of wafer-handling robots.

References

- [1] WU J, LIU P K, WANG Y. Design and analysis of vacuum robot for cluster tools[C]//1st International Conference on Intelligent Robotics and Applications, Wuhan, China, October, 2008: 286–293.
- [2] LEE T E. A review of scheduling theory and methods for semiconductor manufacturing cluster tools[C]//Proceedings of the 40th Conference on Winter Simulation, Miami, Florida, December, 2008: 2 127–2 135.
- [3] TAKASHI K. Vacuum manipulator for semiconductor manufacturing equipment[J]. *Industrial Robot*, 2002, 29(4): 324–328.
- [4] WLODZIMIERZ O. New designs of magnetic fluid exclusion seals for rolling bearings[J]. *Industrial Lubrication and Tribology*, 2005, 57(3): 107–115.
- [5] ZARINA B, BILL W. New low cost ferrofluidic sealing challenges the mechanical seal[J]. *Industrial Lubrication and Tribology*, 1997, 49(6): 288–290.
- [6] BRAS J C M, Vedran A T. Sealing and friction bearing unit containing a magnetic fluid: US, US5100159 [P]. 1992-03-31.
- [7] OZAKI K, FUJIWARA T. Experimental study of high-speed single stage magnetic fluid seals[J]. *Journal of Magnetism and Magnetic Materials*, 1986, 65(2–3): 382–384.
- [8] JIM B. Experimental Study of High speed sealing capability of single stage ferrofluidic Seals[J]. *Journal of Tribology*, 1997, 119(3): 416–421.
- [9] CONG M, ZHOU Y M, JIANG Y, et al. An automated wafer-handling system based on the integrated circuit equipments[C]//IEEE International Conference on Robotics and Biomimetics, ROBIO, Shatin, N.T., China, July 5–9, 2005: 240–245.
- [10] YOSHIO K, TATSUHARU Y, NATSUKI Y, et al. Wafer-handling interface under processing ambient conditions for a single-wafer cluster tool[C]//IEEE Transactions on Semiconductor Manufacturing, Tokyo, Japan, October 2–4, 1996: 13–19.
- [11] HORIGUCHI T. Substrate transporting mechanism, substrate transporting method and substrate processing system: US, 2007/0296134 A1[P]. 2007-3-16.
- [12] SZYDLO Z, OCHONSKI W, ZACHARA B. Experiments on magnetic fluid rotary seals operating under vacuum conditions[J]. *Tribotest*, 2005, 11(4): 345–354.
- [13] MITAMURA Y, ARIOKA S, SAKOTA D, et al. Application of a magnetic fluid seal to rotary blood pumps[J]. *Journal of Physics Condensed Matter*, 2008, 20(20): 204–208.
- [14] RAJ K, MOSKOWITZ B, CASCIARI R. Advances in ferrofluid technology[J]. *Journal of Magnetism and Magnetic Materials*, 1995, 149(1–2): 174–180.
- [15] ROSENWEIG R E. *Ferrohydrodynamics*[M]. Cambridge: Cambridge University Press, 1985.
- [16] YASUNAQA M, KENJI T, KAORU T, et al. Meniscus shape and splashing of magnetic fluid in a magnetic fluid seal[J]. *Journal of Tribology*, 1999, 121(2): 377–383.

- [17] CONG M, DAI P L, SHI H L. A study on wafer-handling robot with coaxial twin-shaft magnetic fluid seals[C]//*2nd International Conference on Intelligent Robotics and Applications, ICIRA 2009*, Singapore, Singapore, December 16–18, 2009: 1 123–1 137.

Biographical notes

CONG Ming, born in 1963, is currently a professor at *School of Mechanical Engineering, Dalian University of Technology, China*. He received his PhD degree in mechanical engineering from *Shanghai Jiaotong University, China*, in 1995. He was a senior engineer of *China HuaLu Group*, and was also an expert of National 863 Plan of China for the development of high technology in the field of robotics. His current research interests include mechanism, robotics, mechanical design, etc. Tel: +86-411-84707147; E-mail: congmdlut.edu.cn

WEN Haiying, born in 1987, is currently a PhD candidate at *School of Mechanical Engineering, Dalian University of*

Technology, China. He received his master degree on mechanical manufacturing in *Dalian University of Technology, China*. His current research interests include vacuum robot technology and optimal design.

E-mail: wenhaiying@gmail.com

DU Yu, born in 1981, is currently a PhD candidate at *School of Mechanical Engineering, Dalian University of Technology, China*. She received her master degree on mechatronics in *Dalian University of Technology, China*, in 2006. Her main research interests include mechatronics, mechanical design, etc.

E-mail: dutdy@yahoo.com.cn

DAI Penglei, born in 1983, is currently an engineer at *Sany Heavy Equipment Co., Ltd, Shenyang, China*. He received his master degree from *Dalian University of Technology, China*, in 2009.

E-mail: daipenglei@yahoo.com.cn